RESPONSE OF A REINFORCED CONCRETE EMBEDDED PILE UNDER LATERAL LOADING. I: FIELD TESTING

E. Ahlberg, J.P. Stewart, J.W. Wallace, C. Rha, E. Taciroglu
University of California, Los Angeles, CA, 90095-1593, USA.

INTRODUCTION

Purpose

Cast-in-drilled-hole (CIDH) shafts are commonly used to provide foundation support to bridge structures due to their ease of installation, cost-effectiveness, and minimal footprint. High-quality experimental data on the full-scale performance of these shafts under lateral and vertical loading is necessary to support the development of reliable analysis and design procedures. This paper reports the results of the second in a series of five tests that subject CIDH foundation systems with various head and geometric conditions to lateral loading.

Test Progression

The first of the five tests was performed on a six-foot diameter shaft in January 2000. Results of this test were reported in Janoyan et al. (2001). The shaft extended 40’ above ground and 48’ below the ground surface. The purpose of the second test was to gauge the effect of reducing the diameter of the column and so was designed with a diameter of 2’ and extended 13’4” above the ground line and 24’ below. The second test was completed in May 2005 and preliminary results are reported herein. The specimen for the third test, a 2’ diameter shaft cast with a large cap at the ground surface, has been constructed and testing is scheduled for October 2005. By controlling the cap rotation using four actuators, the cap will be displaced in a fixed head condition (zero rotation). Comparison of test data from this “fixed-head” condition with results from the second test (a “flagpole” configuration) will enable an assessment of head fixity conditions on the response of otherwise similar shafts. The fourth test will consist of nine shafts identical to the shaft in the third test tied together at the surface by a large pile cap. Comparing the results of the “group” test to the results from the single “fixed-head” shaft will enable an assessment of group effects on the lateral response of shafts. Finally, the fifth test will consist of a pile cap identical to the cap used in the fourth test, but that is not attached to drilled shafts. This test will attempt to capture the lateral passive and frictional resistance of the cap isolated from the drilled shaft contributions.

TEST DESCRIPTION

Site and Soil Characterization

The test site is located on property owned by the California Department of Transportation at the interchange between I-405 and I-105 in the city of Hawthorne, California. The mapped local geology is Quaternary alluvium.

Extensive field and laboratory testing of the site was completed in 1999 and included seismic cone penetration testing (SCPT), rotary-wash borings with standard penetration testing (SPT), down-hole suspension logging of shear wave velocities, pressuremeter testing (PMT), and test pit excavation mapping (Wallace et al., 2001). Figure 1 describes the soil profile and reports relevant laboratory and field test results.

CPT testing was performed in 2004 at the location of the present test specimen and test results indicated that the soil profile is similar to that at the locations investigated in 1999. Based on this finding, we assume that the laboratory results shown in Figure 1 are representative of the soil at the location of the 2'-diameter test.

Drilled Shaft Configuration

The tested shaft consisted of a 24" diameter, spiral reinforced concrete column extending 25' below the ground surface and protruding an additional 13'-4" above ground (See Figure 2). The steel reinforcement consisted of eight #9 longitudinal bars (ρ_s = 0.018) and a #5 spiral at 4" pitch (Figure 2). The longitudinal bars were continuous over the height of the shaft (28'-4" total) and were embedded into the column cap at the top of the shaft. The cap was 30" tall by 24" wide by 8' long and was designed to accept two hydraulic actuators.

The shaft was designed assuming yield strength f_y = 60 ksi for the steel reinforcement and a specified concrete cylinder strength of f_c' = 4 ksi. The results of tests on concrete cylinders cast during shaft construction, and additional specimens cored from the column head, are shown in Figure 3. Ultimate strengths of the tested cylinders were between f_c' = 5.2 and 6.4 ksi, except for one cylinder with f_c' = 4.6 ksi. Presently, steel samples from the reinforcing cage are being prepared for testing and are expected to have yield stresses from 65 to 75 ksi based on data from prior tests.

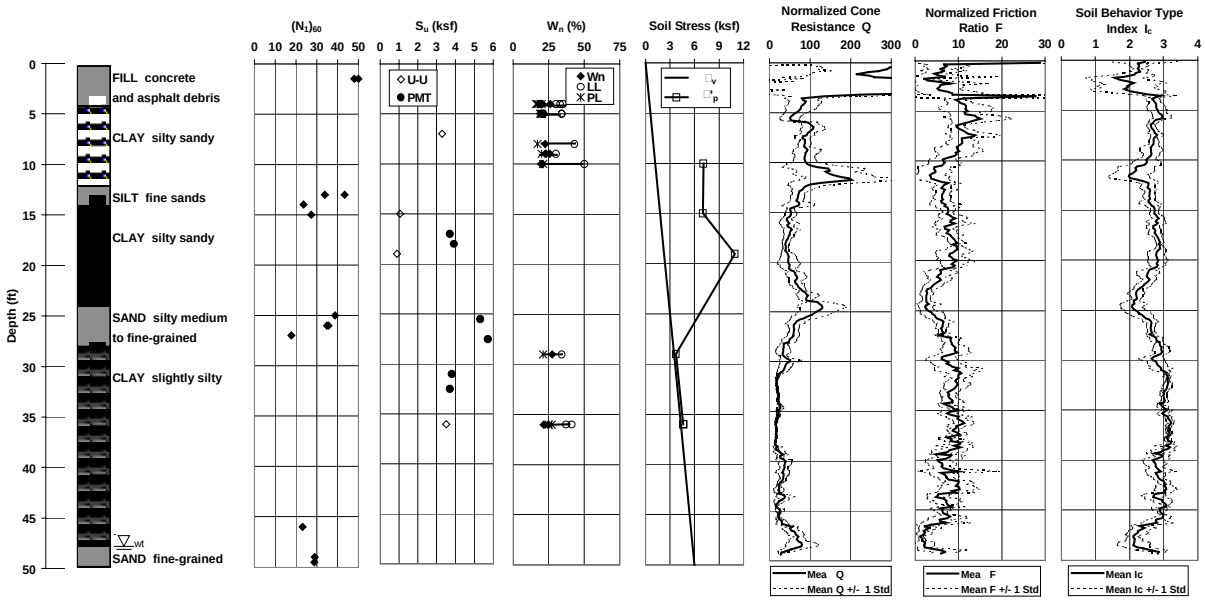

Figure 1: Soil Field and Laboratory Test results

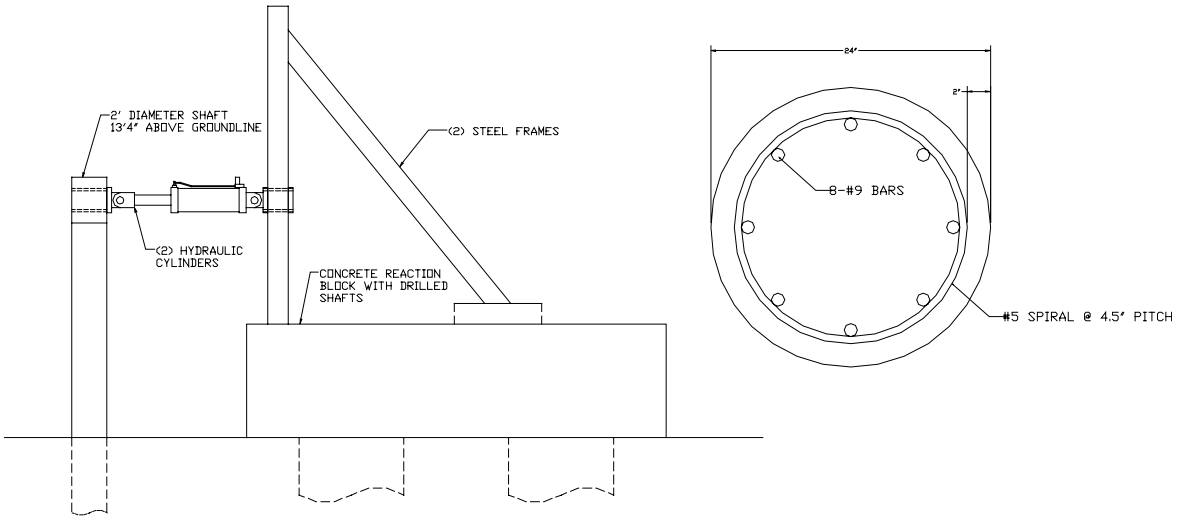

Figure 2: Test Configuration and Reinforcing Details

Load Application System

The load application system consists of a massive concrete reaction structure with a steel reaction frame and two servo-controlled hydraulic actuators. The reinforced concrete reaction structure is a 6' tall by 12' wide by 24' long block at the ground surface supported on two 6'-diameter, 48'-deep concrete CIDH shafts. Several layers of cast hollow tubes that extend over the full length and width of the reaction block allow the actuators to be secured to the reaction system using threaded steel rods. The reaction structure was designed to have a lateral capacity of 3000 kips, well beyond the predicted capacity of any of the test specimens. For the present test, two steel frames were bolted to the top surface of the reaction block to allow the hydraulic actuators to apply horizontal loads to the specimen at a height of 13'4" above the ground surface (See Figure 2).

Two hydraulic actuators were used to load the test specimen. Each actuator has a load capacity of 400 kips (at 3000 psi) and a total stroke of 36". The actuators were controlled by a MTS FlexTest GT controller connected to an IBM ThinkPad laptop running MTS Station Manager control software. The FlexTest GT controller is capable of controlling four actuators based on load, displacement or calculated feedback. Hydraulic power is supplied to the system by a 20-gpm diesel field hydraulic pump, and is regulated by MTS hydraulic service manifolds.

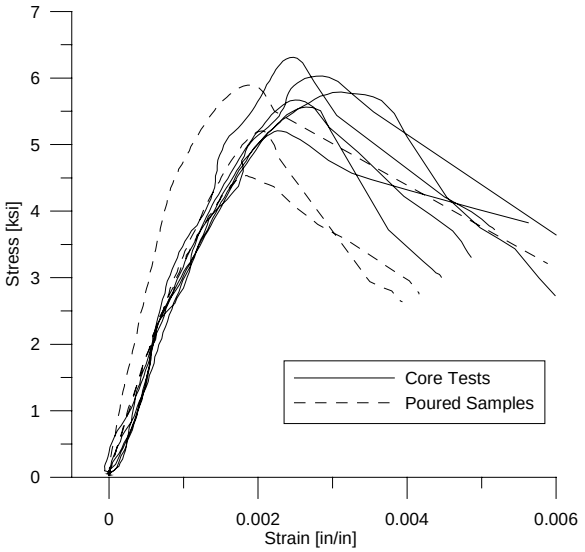

Figure 3: Concrete Compressive Strengths

Instrumentation

Instrumentation was installed in the shaft to measure internal deformations arising from the applied loading at the top of the column. Given the geometry and applied loading condition for the test specimen, flexural deformations were expected to dominate. Accordingly, the majority of the instruments were selected to enable the evaluation of the flexural deformations (e.g., shaft curvature distribution).

The instrumentation layout for this test was guided by analytical predictions of the shaft response (Rha et al, 2005). From the standpoint of instrumentation layout, the key analytical result was the location of maximum moment in the shaft, which was anticipated to be 12 to 30 in. below the ground surface depending on the analysis method. The portion of the shaft predicted to have significant moment was from the ground surface to a depth of 10', with the largest shear forces occurring between the ground surface and 15' depth. Based on these predictions, the test shaft was densely instrumented with four different sensor types to capture flexural and shear responses within this region. Instrumentation was more widely spaced in less critical regions (i.e., at depths below 15 ft, and above ground line). In total, 54 fiber-Bragg gratings (FBGs), 50 DC linear variable displacement transducers (LVDTs), 60 strain gauges, and 11 inclinometers were used to measure the shaft deformations. In addition, pressure transducers measured the applied load and external displacement transducers measured the column lateral displacements at ground line and at the point of load application.

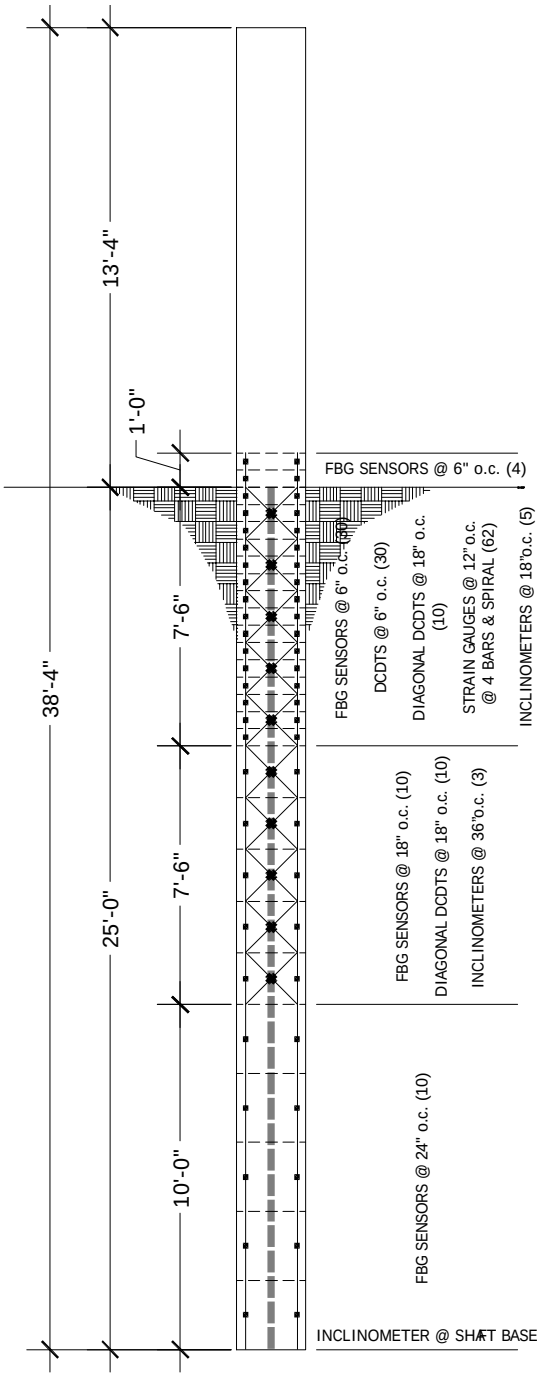

Figure 4: Instrumentation Layout

Fiber-Bragg Gratings

Fiber-optic FBGs, produced by Smartec SA, were installed at 54 locations. FBGs measure average axial concrete strain over a fixed gauge length by recording the shift in the wavelength of light reflected by the grating. The grating consists of a series of etchings in the core of a fiber-optic cable that reflect a very specific and narrow band of light wavelengths. The reflected wavelength depends on the spacing of these etchings, and as the spacing changes with applied strain, the reflected wavelength changes proportionally.

The strain in the concrete specimen is transferred to the FBG via two stainless steel anchors at the ends of each sensor. The fiber is protected from the concrete environment by a plastic casing. The fibers are pre-tensioned to a tensile strain of ~0.5%, which allows the FBG to measure both tensile and compressive strains. With pre-tensioning, the FBGs can measure tensile strains up to about 1% to 1.5%. These sensors also have high resolution (1 microstrain), which allow for accurate strain measurements at low load and deformation levels, which is necessary for accurate assessment of *p-y* relations.

FBGs were placed in pairs normal to the cross-section of the shaft, at the vertical intervals indicted in Figure 4. These 54 sensors were connected to a Micron Optics FBG-SLI swept laser interrogator by a 48 channel switch provided by Smartec SA.

Linear Variable Displacement Transducers

Because the FBG sensors have a limited strain range (~ 2% total strain range), a reducdnat system of LVDTs were deployed to enable measurement of average concrete strains in the areas of the shaft expected to experience large strain. The LVDTs were placed at the same intervals as the 6" gauge length FBGs, allowing the results from each sensor type to be compared. With a stroke of ±1" over the 6" gauge length, the LVDTs were capable of measuring axial strains up to 18%. To protect the LVDTs during concrete placement, they were encased in protective PVC housings that were anchored to the concrete with threaded steel rods. LVDTs were also placed diagonally (in the vertical loading plane) to measure shear deformations. These LVDTs, placed in an "X" pattern, were spaced at 18" from the ground surface to a depth of 15' (See Figure 4).

Strain Gauges

Strain Gauges were placed on four of the longitudinal reinforcing bars and on the spiral reinforcement (Figure 4) to assess the distribution of reinforcement strains within the yielding region of the shaft. The strain gauges were Texas Measurements model YEF gauges with plastic backings that allow them to measure strain at post-yield deformations in the steel bars. The gauges were affixed to the bars using CN-Y adhesive and coated with M-Coat A, M-Coat B, and M-Coat J from Vishay Micromeasurements for water-proofing and protection.

Inclinometers

Eleven Geokon model 6300 inclinometers were installed in the shaft to measure rotation. The locations of inclinometers are shown in Figure 4. Average curvature is obtained by dividing the measured rotation by the gauge length.

Pressure Transducers

In order to measure the load applied at the head of the shaft by the hydraulic actuators, two pressure transducers were installed on each of the two actuators to record fluid pressures on both sides of the piston (the difference in force-area product in each chamber provides the actuator force).

External Displacement Transducers

String-pot displacement transducers were placed at the top of the shaft and near the ground surface to measure the displacement of the shaft relative to an external reference point. One sensor was placed at the centerline of the applied force to give an absolute measurement of the

head displacement of the shaft, while three sensors were placed at 6" vertical intervals above the ground surface to measure displacement, rotation, and curvature of the shaft at that location. Unfortunately, one of the sensors at the ground surface was lost early in the test, which precluded determinations of curvature from external sources at the ground surface.

TEST RESULTS

Testing of the 2'-diameter test specimen began on April 21, 2005 and ended on April 27, 2005. Preliminary results from the tests are summarized in the following subsections.

Loading Regime

The test specimen was loaded using displacement control of the actuators. The specimen was displaced incrementally to increasingly larger displacement levels and cycled three times at each interval. The nominal displacement levels were ±0.25", ±0.5", ±1", ±1.5", ±2", ±2.5", ±3", ±4", ±6", ±8", ±12" and ±16". These displacement levels represent various fractions of the anticipated yield displacement based on the analysis results, which predicted yield displacements between 2.5 to 4.5 in. Actual applied displacements, recorded by the external string-pot displacement transducers, were slightly less due to deflections of the steel reaction frame.

During the first three applied displacement levels to peak values of 0.25", 0.5" and 1", displacements were incremented at ¼ of the peak value, while the subsequent displacement levels were incremented at 1/8 of the peak value (Figure 5). The number of increments was selected to reasonably capture the hysteretic response of the system. Each increment was applied over 30 to 60 sec, using null pacing on the hydraulic controller to ensure that the actuators would displace at the same rate. Each incremental displacement was held for 60 sec to enable data acquisition.

At each displacement level, cracks forming on the above-ground portion of the shaft during the first cycle were marked on the white-washed surface. For subsequent cycles at the same

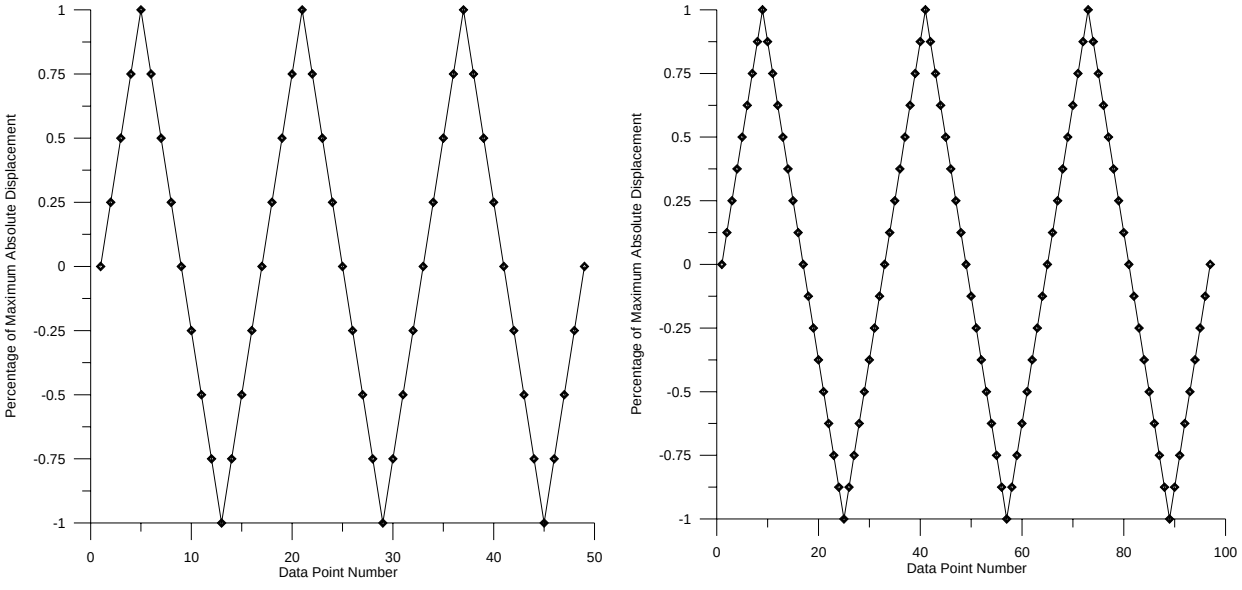

Figure 5: (a) Loading regime and data points for 0.25", 0.5" and 1" displacement levels; (b) all other displacement levels

displacement levels, time-lapse movies of the shaft head were created (http://www.nees.ucla.edu/caltrans/gallery/images/99_Movies/01_2ft_Flagpole/8in_(4_dy)_Disp_Animation.gif) during the second cycle while time-lapse movies of the gap forming at the ground surface were created during the third cycle.

Head Load vs. Head Displacement

The peak head load versus head displacement, or "backbone," curve is shown in Figure 6. In the "South" loading direction, the peak force observed was 28.6 kips while the peak force in the North direction was 23.4 kips. The backbone curves for the two directions diverge for displacements larger than 6"; the cause of this divergence remains under investigation.

Figure 7 displays the load – displacement relations for the specimen at peak displacements of ±0.5" and ±2", respectively. At both displacement amplitudes, the cyclic degradation (from cycle one to cycle three) was small and the hysteretic damping was also small; however, there was significant degradation of shaft stiffness (Figure 7), likely due to concrete cracking.

Curvature Measurements

Curvature profiles for the shaft are generated using compressive and tensile axial strain measurements in the shaft divided by the distance between the locations where these measurements are taken. The fiber-optic and strain gauges measure average axial strain directly, while axial strains are calculated from LVDT measurements by dividing displacements by the gauge length. Curvatures are calculated from inclinometer measurements by dividing the difference between measured rotations by the inclinometers gauge length.

Figure 8 shows curvature profile data from fiber-optic sensors over the depth of the shaft at the ±0.5" and ±2" displacement levels. At the 0.5" displacement level, the maximum curvature of 0.000021/inch in the South direction and 0.000038/inch in the North direction occurred near the ground surface. At the 2" displacement level, the maximum curvature of 0.00016/inch in the South direction and 0.00017/inch in the North direction occurred approximately 20" below the

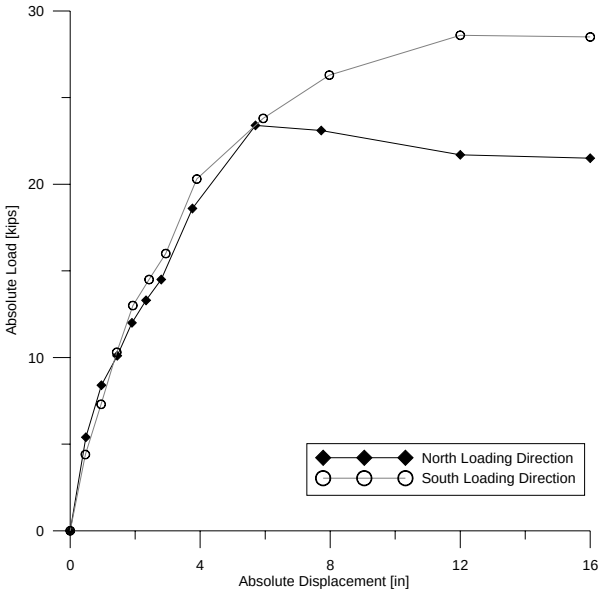

Figure 6: North and South Backbone Curves

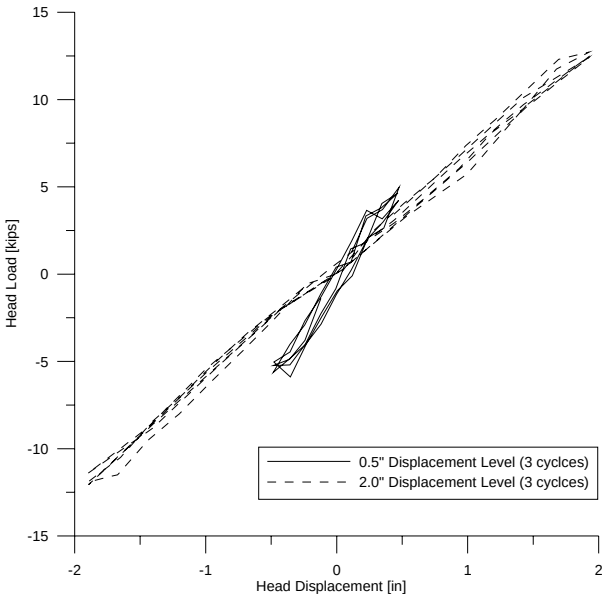

Figure 7: Hysteresis for 0.5" and 2" Displacements

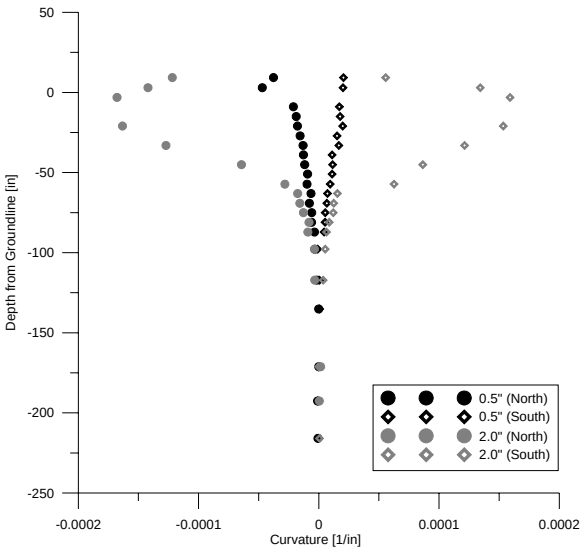

Figure 8: 0.5" & 2.0" Disp. Curvature Profiles

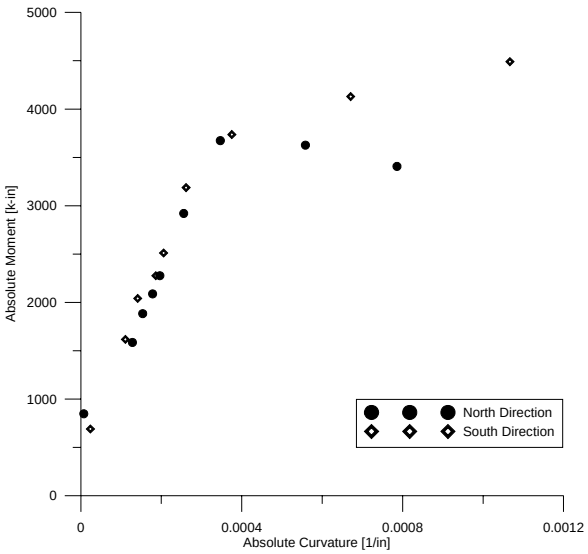

Figure 9: Experimental Moment-Curvature

ground surface. The location of the maximum curvature (and accordingly, the maximum moment) continued to migrate downward at higher displacement levels. Post-test investigations of the shaft indicated that longitudinal reinforcing bars eventually fractured at about 3.5' below the ground surface. The experimental moment-curvature relationship is shown in Figure 9.

SIGNIFICANCE OF THE DATA AND FUTURE WORK

The curvature profiles generated from four different sensor types allow *p-y* curves and their associated uncertainties to be calculated. Once the sensor data are fully reduced and analyzed, uncertainties associated with sensor variations and local shaft deformations will be more completely quantified. An appropriate regression fit through the curvature data will allow the curvature and moment profiles to be used to produce *p-y* curves. This same statistical process will also be applied to data from the previous 6 ft diameter test (Janoyan et al., 2001) to evaluate diameter effects on *p-y* curves.

REFERENCES

Janoyan, K., Stewart, J.P., and Wallace, J.W. (2001). "Analysis of p-y curves from lateral load test of large diameter drilled shaft in stiff clay," *Caltrans 6th Seismic Design Workshop*, Sacramento, CA. Paper 5-105.

Rha, C., Taciroglu, E., Ahlberg, E., Wallace, J.W., Stewart, J.P. (2005) "Response of a reinforced concrete embedded pile under lateral loading. II: Numerical studies," *2005 Caltrans Bridge Research Conference*, Sacramento, CA, Paper 8-504.

Wallace, J.W., Fox, P.J., Stewart, J.P., Janoyan, K., Qiu, T., and Lermitte, S. (2001). "Cyclic large deflection testing of shaft bridges. Part I-Background and field test results," Report to California Department of Transportation, December. Available at http://cee.ea.ucla.edu/CT-foundations/